る[3]。最近、さらに日本人から新たにアミノ酸置換を伴う *CYP2C8*X* 及び *CYP2C8*Y* が見出されている。

本研究では SU 剤の薬効と HNF4A(1-Mutant 及び 2-Mutant)あるいは CYP2C8 の遺伝子多型の関連性を明確にし、SU 剤の適正投薬法を確立することを目的として、変異型 HNF4A(1型及び2型)の転写活性並びに変異型 CYP2C8 の酵素機能について追究した。

B. 実験方法

試薬

実験に用いた試薬などの入手先は以下に示す。PolyFect Transfection Reagent : Qiagen ; Dual-Glo Luciferase Assay System, pGEM-T ベクター : Promega ; ヒト肝全 RNA, 6α-ヒドロキシパクリタキセル : BD Biosciences ; KOD-plus DNA polymerase : Toyobo ; *Hin*dIII : Takara Bio ; BigDye terminator cycle sequencung reaction kit v3.1 : Applied Biosystems ; QuikChange site-directed mutagenesis kit : Stratagene ; Yeast nitrogen base : BD Diagnostics ; Zymolyase 100T : 生化学工業 ; パクリタキセル : 和光純薬工業 ; ドセタキセル : Sigma-Aldrich ; NADPH, glucose 6-phosphate (G-6-P), glucose 6-phosphate dehydrogenase (G-6-PDH) : オリエンタル酵母 ; PVDF 膜 : BioRad ; ウサギ抗ヒト CYP2C8/9/19/12 抗体 : Chemicon ; ペルオキシダーゼ標識ヤギ抗ウサギ IgG : Zymed Laboratories ; ECL plus reagent : GE Healthcare BioSciences; HNF4A (1型及び2型) (Blank, 1-WT, 1-Mutant, 2-WT 及び 2-Mutant) cDNA を挿入した pcDNA3.2-DEST ベクター(pcDNA3.2-DEST/HNF4A), HNF1A のプロモーター領域(HNF4A 結合部位を含む)を挿入した pGL3-Basic ベクター (pGL3-Basic/promoter),phRL-TK ベクター,COS-7 細胞及び;ウサギ抗ヒト HNF4A 抗体は斎藤嘉朗博士(国立医薬品食品衛生研究所)から供与された。pGYR I 酵母細胞発現ベクター及び *Saccharomyces cerevisiae* AH22 株は舩江良彦教授(大阪市立大学大学院医学研究科)から供与された。その他試薬は分析用、特級及び HPLC 用試薬を購入した。

COS-7 細胞の培養及び HNF4A プラスミドのトランスフェクション

COS-7 細胞は 37℃、95% O_2/5% CO_2 の気相下において 10% FBS、penicillin (100 U/ml)及び streptomycin (100 μg/ml)含有 DMEM 培地中に培養した。

ウエスタンブロッティングによる HNF4A タンパク質発現確認では、100 mm プレートに細胞が $1.6x10^6$ cells となるように継代し、24 時間培養した。次に PolyFect Transfection Reagent を用いてプロトコールに従ってそれぞれの pcDNA3.2-DEST/HNF4A を細胞にトランスフェクションした。さらに 24 時間培養し、細胞を 1/50 量のプロテアーゼインヒビターを含む緩衝液(50 mM Kpi buffer (pH 7.4)-0.25 M sucrose-25 mM KCl)で懸濁し、ライセート画分を調製した。調製したライセート画分は、使用するまで-80°C で保存した。

デュアルルシフェラーゼレポーターアッセイによる HNF4A 転写活性測定では、6 ウェルプレートに細胞が $4.0x10^4$ cells となるように継代し、24 時間培養した。次に PolyFect Transfection Reagent を用いて pcDNA3.2-DEST/HNF4A 、 pGL3-Basic/promoter 及び phRL-TK を細胞に同時トランスフェクションした。さらに 24 時間培養した後、Dual-Glo Luciferase Assay System を用いてプロトコールに従ってそれぞれの HNF4A の転写活性を測定した。転写活性はそれぞれの細胞におけるホタルルシフェラーゼ活性(Fluc)とウミシイタケルシフェラーゼ活性(Rluc)の比(Fluc/Rluc)として表した。

野生型及び変異型 CYP2C8 プラスミドの作製

CYP2C8*1A cDNA のクローニングはヒト肝全 RNA からの PCR 法により行った。まず、ヒト全 RNA から RNA PCR kit (AMV) v3.0 を用いて逆転写反応により一本鎖 cDNA を合成した。CYP2C8*1A cDNA は、セ

ンスプライマーとして 5′-AAGCTTAAAAAAATGGAACCTTTTGTGGTCCTGG-3′、アンチセンスプライマーとして 5′-AAGCTTTTCAGACAGGGATGAAGCAGATC-3′ を用い、50 ng のヒト肝一本鎖 cDNA を鋳型にして PCR 反応により増幅した。センス及びアンチセンスプライマーの 5′末端には pGYR1T ベクターにサブクローニングするための *Hin*dIII 認識配列(下線)を付加した。また、センスプライマーには酵母コンセンサス配列(波線)を付加した。PCR は、1 U KOD-plus DNA polymerase、1 mM $MgSO_4$、0.2 mM dNTPs 及び 0.5 μM プライマーセット(センス及びアンチセンスプライマー)を含む反応組成(50 μl)で行った。PCR は、94℃で 2 分間変性させた後、94℃で 30 秒間(変性)、65℃で 30 秒間(アニーリング)、68℃で 100 秒間(伸長反応)を行った。反応液をアガロースゲル電気泳動に付し、PCR 産物を精製した。次に、その PCR 産物の 3′末端に A を付加するために、PCR 産物(1 μL)、25 mM $MgCl_2$、2 mM dATP 及び 1 U/μL r-Taq polymerase を含む全量 10μl の反応液で 72℃、30 分間反応させた。A 付加後の PCR 産物(2 μl)を用いて 3 U T4 DNA ligase により pGEM-T vector(50 ng)と 4℃で 16 時間ライゲーションした。ヒートショック法により得られたプラスミド DNA で *Escherichia coli* DH5α を形質転換した。形質転換後のコロニーの選択は *lac*Z 遺伝子に基づくカラーセクションにより行った。CYP2C8*1A cDNA の配列は BigDye terminator cycle sequencing reaction kit v3.1 を用いたシーケンシングにより確認した(pGEM-T/CYP2C8*1A)。

CYP2C8*X 及び CYP2C8*Y cDNA は pGEM-T/CYP2C8*1A を鋳型にして部位特異的変異導入法により作製した。目的部位への変異の導入の成否は BigDye terminator cycle sequencung reaction kit v3.1 を用いてシーケンシングにより確認した。

pGEM-T/CYP2C8s cDNA を制限酵素 *Hin*dIII で完全消化(37℃、24 時間)後、エタノール沈殿を行って DNA を精製し、インサート DNA 溶液を調製した。また、pGYR I ベクターも *Hin*dIII で完全消化し、ベクターのセルフライゲーションを防ぐため、アルカリフォスファターゼ(CIAP)を用いて 37℃で 4 時間反応させ、5′-末端リン酸基を除去した。次に、野生型及び変異型 CYP2C8 cDNA を pGYR I の *Hin*dIII 切断部位に、16℃で 16 時間ライゲーションし、塩化カルシウム法により *Echerichia coli* DH5α を形質転換した。目的 cDNA の挿入及び pGYR I ベクターの発現プロモーターに対する挿入方向はシーケンシングにより確認した。

CYP2C8 酵素の発現

酵母細胞の形質転換は、Ito らの方法[4]に従って行った。すなわち、YPD 培地[1% Bacto yeast extract、2% Tryptone peptone、2% D-(+)-Glucose]2 mL で *Saccharomyces cerevisiae* AH22 株を 30℃で振盪培養し、YPD 培地 5 mL に植菌後、対数増殖期(OD_{660}=0.6–1.0)まで振盪培養した。その酵母細胞液 1 mL を 4℃、2,000×g で 2 分間遠心して集菌し、0.1 M 塩化リチウム 1 mL で懸濁した後、同条件で遠心した。得られた菌体を 1 M 塩化リチウム 20 μL で懸濁し受容菌とした。この受容菌にプラスミド DNA(pGYR I /CYP2C8s)及び 70%ポリエチレングリコール溶液 30 μL を加え穏やかに懸濁後、30℃で 1 時間静置した。次いで滅菌精製水 140 μL を加えて希釈し、SDH 寒天培地[0.67% Yeast nitrogen base w/o amino acids、8% D-(+)-Glucose、0.02% L-Histidine、1.5% Agar]に蒔き、30℃で 72 時間培養した。培養後、Wan らの方法[5]に従い得られたコロニーを SDH 液体培地[5.4% Yeast nitogen base w/o amino acids、8% D-(+)-Glucose、0.02% Histidine]に植菌し、30℃で 60 時間振盪培養した。その酵母培養液 1 mL を SDH 液体培地 10 mL に植菌し、同条件下 24 時間振盪培養した。次いで、その酵母培養液 5 mL を SDH 液体培地 200 mL に植菌し、同条件下 24 時間振盪培養した。さらにその全量を 1.8 L の SDH 液体培地に植菌し、pH 5.5、好気的条件下で 24 時間培養した。

CYP2C8 酵母発現ミクロソーム画分の調製

Hichiya らの方法[6]に準じて行った。上記酵母培養液を 2,000×g で 20 分間遠心し、得られた菌体を氷冷した超純水で懸濁後、再度同条件で遠心した。上清を除去し、菌体を Solvent A[10 mM Tris-HCl、2 M D-Glucitol、0.1 mM DTT、0.2 mM EDTA (pH 7.4)]で懸濁後、同条件で遠心した。上清を除去し、菌体を 50 U/mL zymolyase 含有 SolventA で穏やかに懸濁し 35℃で 90 分間振盪した後、2,000×g で 10 分間遠心した。上清を除去し、菌体をプロテアーゼ阻害剤(1 mM EDTA、1 mM PMSF、0.1 μM アプロチニン、0.1 μM ロイペプチン)を含む Solvent B[10 mM Tris-HCl、0.65 M D-Glucitol、0.1 mM EDTA (pH 7.4)]で穏やかに懸濁後、超音波細胞粉砕器(日立精機製作所)を用いて 30 秒間、5 分間隔で 10 回細胞破壊を行った。得られたライセートを 9,000×g で 30 分間遠心分離し、上清を 105,000×g で 60 分間遠心分離した。得られた沈殿に 1 mM EDTA、1 mM DTT、20%グリセロール含有 100 mM NaH_2PO_4(pH 7.4)を加えホモジナイズし、ミクロゾーム画分を調製した。得られたミクロゾーム画分は使用するまで-80℃で保存した。陰性対照として pGYR I のみをトランスフェクションしたものを同様に作製した(mock)。ミクロゾーム画分のタンパク質量は Lowry らの方法[7]に従って牛血清アルブミンを標準物質として定量した。

還元型 CO 差スペクトルの測定

酵母細胞ミクロソーム画分を Buffer D[100 mM phosphate buffer (pH 7.4)-0.4% Emulgen911-20% glycerol]に懸濁し(10 mg/ml)、Omura と Sato の方法[8]に従って吸収スペクトルを測定した。希釈した試料 1 ml ずつを試料セル及び対照セルに入れ、400～500 nm 間のベースラインを補正した。次いで試料セルのみに一酸化炭素を通じ、両セルに約 1 mg のハイドロサルファイトナトリウムを加え穏やかに混和した後、400～500 nm 間のスペクトルを記録した。得られた 450 及び 490 nm の吸光度差より吸光度係数 91 $mM^{-1}cm^{-1}$ を用いて CYP 含量を算出した。

ウェスタンブロット分析

酵母ミクロソームを Laemmli らの方法[9]に準じて 10% SDS-ポリアクリルアミドゲル電気泳動に付した。泳動後、Towbin らの方法[10]に従いタンパク質を PVDF 膜に転写した。PVDF 膜は一次抗体としてウサギ抗ヒト HNF4A 抗体あるいはウサギ抗ヒト CYP2C8/9/19/12 抗体を、二次抗体としてペルオキシダーゼ標識ヤギ抗ウサギ IgG を加え、室温でインキュベートした。洗浄後、抗体と結合したタンパク質を化学発光法により検出した。

パクリタキセル 6α-水酸化活性の測定

パクリタキセル 6α-水酸化活性は、Soyama らの方法[11]に準じて測定した。

	Final concentration
Kpi buffer (pH 7.4)	50 mM
$MgCl_2$	10 mM
G-6-P	10 mM
G-6-PDH	0.5 U/mL
EDTA	0.2 mM
Paclitaxel	10 μM
Microsomes	2000 μg protein/mL
NADPH	1 mM
Total volume	500 μL

CYP2C8 発現酵母ミクロゾームを除く上記の反応混合液を、37℃で 1 分間予備反応した後、CYP2C8 発現酵母ミクロゾームの添加によって反応を開始した。37℃で 10 分間反応した後、酢酸エチルを 3 mL 添加して反応を停止した。内部標準物質としてドセタキセル(10 nmol)を加えて 2 分間激しく撹拌した後、2,500×g で 10 分間遠心分離した。その有機溶媒相を分取し、窒素ガス気流下(35℃)で乾固した。残渣は 400 μL の 50% methanol に溶解し、その内の 50 μL を HPLC に付し、6α--ヒドロキシパクリタキセル生成量を内部標準法にて算出した。パクリタキセルは DMSO:metanol(50:50, v/v)に溶解し、この反応液中の有機溶媒濃度は 1%とした。HPLC 条件は下記のように設定した。

Column: Inertsil ODS 80A (4.6 mm i.d. × 150 mm)

Column temperature: 40°C
Elution: Water-methanol-acetonitrile
(52:34:114, v/v/v)
Flow rate: 1.2 mL/min
Detection: UV 230 nm

C. 結果

COS-7 細胞における野生型及び変異型 HNF4A タンパク質の発現

COS-7 細胞で発現させた HNF4A タンパク質(1-WT、1-Mutant、2-WT 及び 2-Mutant)の細胞ライセート画分の発現をウェスタンブロット分析により確認した。その結果を Fig. 1 に示す。陰性対照(Blank)を除くいずれの HNF4A 発現ライセートにおいても抗ヒト HNF4A 抗体と強く交差するバンドが検出された。なお、陽性対照として HepG2 細胞ライセートを用いた。

野生型及び変異型 HNF4A の転写活性

COS-7 細胞に pcDNA3.2-DEST/HNF4A と共に HpGL3-Basic/promoter 及び phRL-TK ベクターをトランスフェクションし、デュアルルシフェラーゼレポーターアッセイにより野生型及び変異型 HNF4A(1型及び2型)の転写活性(Fluc/Rluc)を測定した。その結果を Fig. 2 に示す。HNF4A の1型及び2型のいずれにおいても転写活性に野生型と変異型の間で有意な差は認められなかった(1型, P=0.059;2型, P=0.136)。

酵母細胞における野生型及び変異型 CYP2C8 タンパク質の発現

酵母細胞で発現させた野生型及び変異型 CYP2C8 酵素タンパク質の細胞ミクロゾーム画分の発現量をウェスタンブロット分析により確認した。その結果を Fig. 3 に示す。陰性対照を除く野生型及び変異型いずれの CYP2C8 酵母細胞発現ミクロゾームにおいても抗ヒト CYP2C8/9/19/12 抗体と交差するバンドが検出された。CYP2C8.X 及び CYP2C8.Y の相対的バンド強度は野生型とほぼ同程度であった。また、CYP2C8 発現酵母細胞ミクロゾームを用いて還元型 CO 差スペクトルによる CYP 含量の測定を行った。その結果を Fig. 4 に示す。野生型及び CYP2C8.X では 450 nm に吸収極大が認められ、機能性 CYP 含量はそれぞれ 26.4 及び 10.6 pmol/mg protein であった。一方、CYP2C8.Y では 450 nm における吸収極大のピークは全く認められなかった。

野生型及び変異型 CYP2C8 酵素の機能

野生型及び変異型 CYP2C8 の酵素機能を解析するために、CYP2C8 発現酵母細胞ミクロゾームのパクリタキセル 6α-水酸化活性を測定した。その結果を Fig. 5 に示す。野生型 CYP2C8 の基質濃度 10 μM におけるパクリタキセル 6α-水酸化活性は、4.68 pmol/min/CYP であった。CYP2C8.X の活性は野生型 CYP2C8 とほぼ同程度であったが、CYP2C8.Y では全く活性は検出されなかった。

D. 考察

本研究は SU 剤の適正投薬法を確立するための一環として、日本人で新たに見出された変異型 HNF4A(1型及び2型)の転写活性並びに変異型 CYP2C8 の酵素機能について検討した。HNF4A は COS-7 細胞に、CYP2C8 は酵母細胞に発現させた。

HNF4A 発現 COS-7 細胞ライセートのウェスタンブロット分析において、野生型(1-WT 及び 2-WT)及び変異型(1-Mutant 及び 2-Mutant)のいずれにおいても抗ヒト HNF4A 抗体と免疫交差するバンドが認められた。次に、野生型あるいは変異型 HNF4A プラスミドと共に HNF1A のプロモーター領域(HNF4A 結合部位を含む)を挿入したプラスミド及びウミシイタケルシフェラーゼ発現プラスミドを COS-7 細胞にトランスフェクションしてそれぞれの野生型及び変異型 HNF4A(1型及び2型)の転写活性を測定した。HNF4A の1型及び2型のいずれにおいても転写活性に野生型と変異型の間で有意な差は認められず、HNF4A における 1154C>T (A385V) 及び 1193T>C (M398T)の一塩基多型は

転写活性に顕著な影響を与えないことが示唆された。

CYP2C8 発現酵母細胞ミクロゾームのウェスタンブロット分析において、野生型及び変異型(CYP2C8.X 及び CYP2C8.Y)のいずれにおいても抗ヒト CYP2C8/9/19/12 抗体と免疫交差するバンドが認められた。一方、還元型 CO 差スペクトルにおいては、野生型及び CYP2C8.X では 450 nm に吸収極大が認められたが、CYP2C8.Y ではそのピークは検出されなかった。また、CYP2C8.X の機能性 CYP 含量は野生型の約 40%であった。このウェスタンブロット分析と還元型 CO 差スペクトルにおける結果の相違の原因は不明であるが、酵母細胞での酵素タンパク質発現の過程におけるそれぞれの転写/翻訳効率、あるいは発現タンパク質の折りたたみ構造の安定性の違いによる可能性が考えられる[12,13]。さらに、野生型及び変異型 CYP2C8 の酵素機能を検証するためにそれぞれの CYP2C8 発現酵母細胞ミクロゾームを酵素源にしてパクリタキセル 6α-水酸化活性を測定した。CYP2C8.X は野生型 CYP2C8 とほぼ同程度の活性を示したが、CYP2C8.Y はパクリタキセルに対する 6α-水酸化活性を全く有していなかった。この現象は、還元型 CO 差スペクトルの結果を概ね反映したものと思われる。また、CYP2C8*Y におけるアミノ酸置換部位はパクリタキセルに対する代謝能を規定する重要なアミノ酸残基であることが示唆された。

E. 総括

本研究では、日本人で新たに見出された変異型 HNF4A(1型及び2型)の転写活性並びに変異型 CYP2C8 の酵素機能について検討した。COS-7 細胞にトランスフェクションした HNF4A の1型及び2型の転写活性は、いずれも野生型(1-WT; 2-WT)と変異型(2-Mutant; 2-Mutant)の間で有意な差は認められなかった。CYP2C8 のパクリタキセル 6α-水酸化活性は、CYP2C8.X では野生型比べてほぼ同程度であったのに対し、CYP2C8.Y ではその活性は完全に欠損していた。この結果は、CYP2C8.Y におけるアミノ酸置換が CYP2C8 酵素の機能を顕著低下させることを示唆しており、*CYP2C8*Y* は医薬品の薬効及び副作用発現に何らかの影響を及ぼす変異型遺伝子である可能性が考えられた。

F. 参考文献

[1] Fukushima-Uesaka H, Saito Y, Maekawa K, Saeki M, Kamatani N, Kajio H, Kuzuya N, Yasuda K, Sawada J. Novel genetic variations and haplotypes of hepatocyte nuclear factor 4α (HNF4A) found in Japanese type II diabetic patients. Drug Metab Pharmacokinet 2006;21:337–46.

[2] Martínez-Jiménez CP, Castell JV, Gómez-Lechón MJ, Jover R. Transcriptional activation of CYP2C9, CYP1A1, and CYP1A2 by hepatocyte nuclear factor 4α requires coactivators peroxisomal proliferator activated receptor-gamma coactivator 1alpha and steroid receptor coactivator 1. Mol Pharmacol 2006;70:1681–92.

[3] Rendic S, Di Carlo FJ. Human cytochrome P450 enzymes: a status report summarizing their reactions, substrates, inducers, and inhibitors. Drug Metab Rev 1997;29:413–580.

[4] Ito H, Fukuda Y, Murata K Kimura A. Transformation of intact yeast cells treated with alkali cations. J Bacteriol 1983;153:163–8.

[5] Wan J, Imaoka S, Chow T, Hiroi T, Yabusaki Y Funae Y. Expression of four rat CYP2D isoforms in Saccharomyces cerevisiae and their catalytic specificity. Arch Biochem Biophys 1997;348:383–90.

[6] Hichiya H, Takemi C, Tsuzuki D, Yamamoto S, Asaoka K, Suzuki S, Satoh T, Shinoda S, Kataoka H Narimatsu S. Complementary DNA cloning and characterization of cytochrome P450 2D29 from Japanese monkey liver. Biochem Pharmacol 2002;64:1101–10.

[7] Lowry OH, Rosebrough NJ, Farr AL, Randall RJ. Protein measurement with the Folin phenol reagent. J Biol Chem 1951;193:265–75.

[8] Omura T, Sato R. The carbon monooxide-binding pigment of liver microsomes. I.

Evidence for its hemoprotein nature. J Biol Chem 1964;239:2370–78.

[9] Laemmli UK. Cleavage of structural proteins during the assembly of the head of bacteriophage T4. Nature 1970;227:680–85.

[10] Towbin H, Staehelin T Gordon J. Electrophoretic transfer of proteins from polyacrylamide gels to nitrocellulose sheets: procedure and some applications. Proc Natl Acad Sci USA 1979;76:4350–54.

[11] Soyama A, Saito Y, Hanioka N, Murayama N, Nakajima O, Katori N, Ishida S, Sai K, Ozawa S, Sawada J. Non-synonymous single nucleotide alterations found in the CYP2C8 gene result in reduced *in vitro* paclitaxel metabolism. Biol Pharm Bull. 2001;24:1427–30.

[12] Johansson I, Oscarson M, Yue QY, Bertilsson L, Sjoqvist F, Ingelman-Sundberg M. Genetic analysis of the Chinese cytochrome P4502D locus: characterization of variant CYP2D6 genes present in subjects with diminished capacity for debrisoquine hydroxylation. Mol Pharmacol 1994;4:452–59.

[13] Fukuda T. Nishida Y, Imaoka S, Hiroi T, Naohara M, Funae Y, Azuma J. The decreased *in vivo* clearance of CYP2D6 substrate by CYP2D6*10 might be caused not only by the low-expression but also by low affinity of CYP2D6. Arch Biochem Biophys 2000;380:303–8.

G. 健康危険情報

なし。

H. 研究発表

1. 論文発表

1) Hanioka N, Tsuneto Y, Saito Y, Sumada T, Maekawa K, Saito K, Sawada J, Narimatsu S. Functional characterization of two novel CYP2C19 variants (*CYP2C19*18* and *CYP2C19*19*) found in a Japanese population. Xenobiotica 2007;37:342–55.

2) Saito K, Dan H, Masuda K, Katsu T, Hanioka N, Yamamoto S, Miyano K, Yamano S, Narimatsu S. Stereoselective hexobarbital 3′-hydroxylation by CYP2C19 expressed in yeast cells and the roles of amino acid residues at positions 300 and 476. Chirality 2007;19:550–8.

3) Hanioka N, Tsuneto Y, Saito Y, Maekawa K, Sawada J, Narimatsu S. Influence of *CYP2C19*18* and *CYP2C19*19* alleles on omeprazole 5-hydroxylation: in vitro functional analysis of recombinant enzymes expressed in Saccharomyces cerevisiae. Basic Clin Pharmacol Toxicol 2008;102:388-393.

2. 学会発表

[1] 中田晋太郎, 斎藤嘉朗, 佐伯真弓, 澤田純一, 埴岡伸光, 成松鎭雄:ヒト HNF4α を介した転写活性化に及ぼす SHP の影響. 第 46 回日本薬学会・日本薬剤師会・日本病院薬剤師会中国四国支部学術大会, 高知, 2007 年 11 月.

G. 知的財産権の出願・特許

なし。

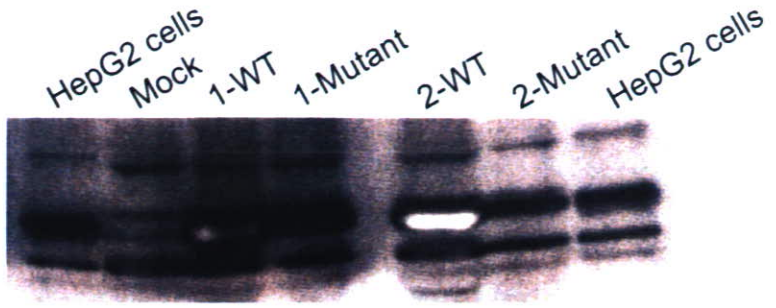

Fig. 1. Western blot analysis of lysates from COS-7 cells expressing wild-type and variant HNF4As. The lysate protein level applied was 20 μg/lane.

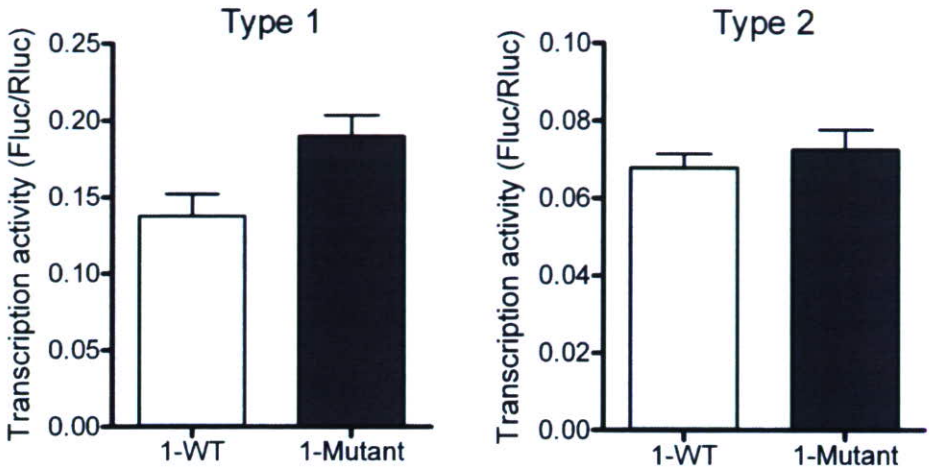

Fig. 2. Transcription activities of wild-type and variant HNF4As expressed in COS-7 cells.

Fig. 3. Western blot analysis of microsomes from yeast cells expressing wild-type and variant CYP2C8s. The microsomal protein level applied was 10 μg/lane.

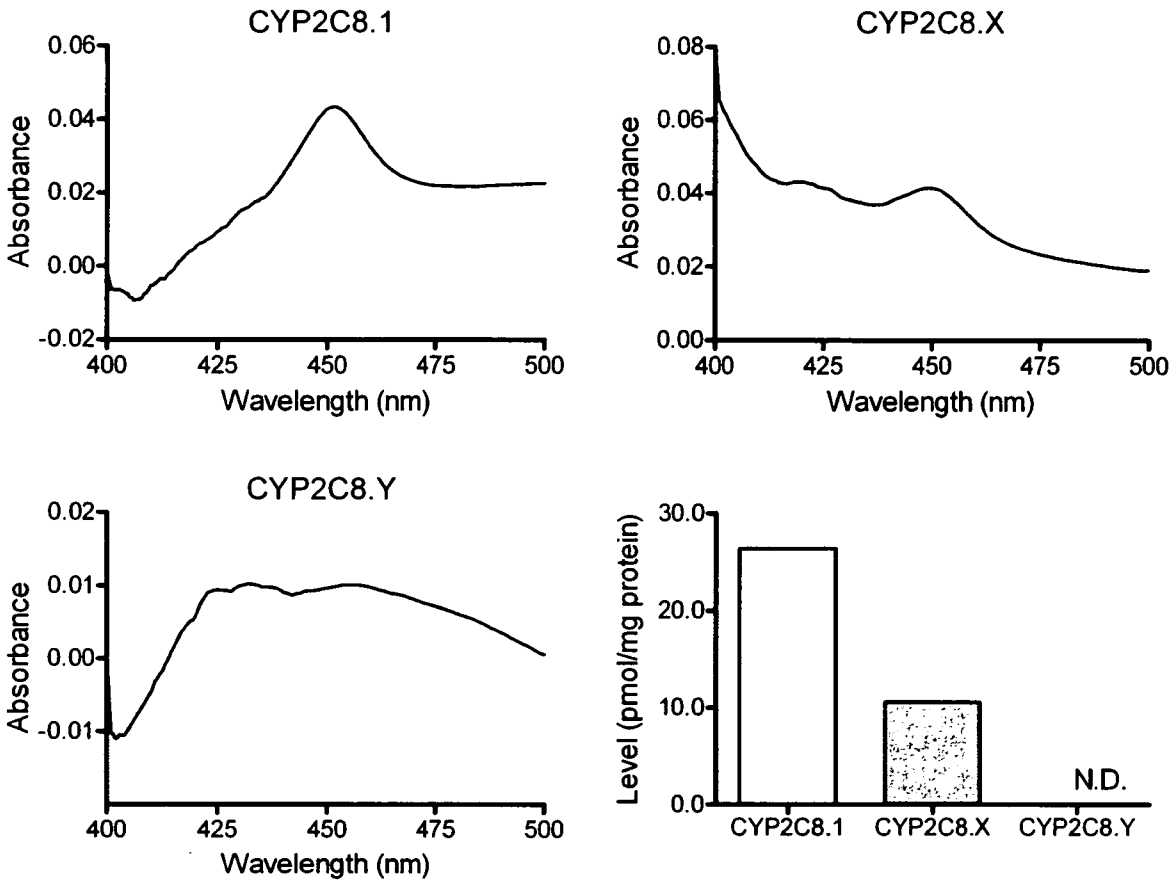

Fig. 4. Reduced CO-difference spectra of microsomes from yeast cells expressing wild-type and variant CYP2C8s. The microsomal protein concentration used was 10 mg/mL. Bar graph represents the expression levels of CYP2C8.

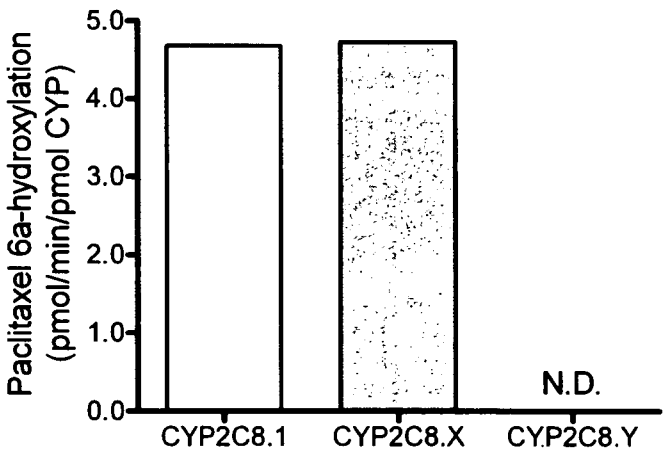

Fig. 5. Paclitaxel 6α-hydroxylation activities in microsomes from yeast cells expressing wild-type and variant CYP2C8s. The substrate concentration used was 10 μM.

別添５

III. 研究成果の刊行に関する一覧表

研究成果の刊行に関する一覧表

雑誌

発表者氏名	論文タイトル名	発表誌名	巻号	ページ	出版年
Hanioka N, Tsuneto Y, Saito Y, Sumada T, Maekawa K, Saito K, Sawada J, Narimatsu S.	Functional characterization of two novel CYP2C19 variants (*CYP2C19*18* and *CYP2C19*19*) found in a Japanese population.	Xenobiotica	37	342-355	2007
Fukushima-Uesaka H, Saito Y, Maekawa K, Hasegawa R, Suzuki K, Yanagawa T, Kajio H, Kuzuya N, Noda M, Yasuda K, Tohkin M, Sawada J.	Genetic variations of the ABC transporter gene ABCC3 in a Japanese population.	Drug Metab. Pharmaco-Kinet.	22	129-135	2007
Fukushima-Uesaka H, Saito Y, Maekawa K, Kamatani N, Kajio H, Kuzuya N, Noda M, Yasuda K, Sawada J.	Genetic variations and haplotype structures of a transcriptional factor Nrf2 and its cytosolic reservoir protein Keap1 in Japanese.	Drug Metab. Pharmaco-Kinet.	22	212-219	2007
Saito K, Dan H, Masuda K, Katsu T, Hanioka N, Yamamoto S, Miyano K, Yamano S, Narimatsu S.	Stereoselective hexobarbital 3´-hydroxylation by CYP2C19 expressed in yeast cells and the roles of amino acid residues at positions 300 and 476.	Chirality	19	550-558	2007
Takeuchi F, Yanai K, Inomata H, Kuzuya N, Kajio H, Honjo S, Takeda N, Kaburagi Y, Yasuda K, Shirasawa S, Sasazuki T, Kato N.	Search of type 2 diabetes susceptibility gene on chromosome 20q.	Biochem. Biophys. Res. Commun.	357	1100-1106	2007
Hanioka N, Tsuneto Y, Saito Y, Maekawa K, Sawada J, Narimatsu S.	Influence of *CYP2C19*18* and *CYP2C19*19* alleles on omeprazole 5-hydroxylation: in vitro functional analysis of recombinant enzymes expressed in Saccharomyces cerevisiae.	Basic Clin. Pharmacol. Toxicol.	102	388-393	2008
Takeuchi F, Ochiai Y, Serizawa M, Yanai K, Kuzuya N, Kajio H, Honjo S, Takeda N, Kaburagi Y, Shirasawa S, Sasazuki T, Kato N.	Search for type 2 diabetes susceptibility genes on chromosome 1q, 3q and 12q.	J. Hum. Genet.		in press	

Ⅳ．研究成果の刊行物・別刷

Xenobiotica, April 2007; 37(4): 342–355

Functional characterization of two novel CYP2C19 variants (*CYP2C19*18* and *CYP2C19*19*) found in a Japanese population

N. HANIOKA[1,*], Y. TSUNETO[1,*], Y. SAITO[2], T. SUMADA[1], K. MAEKAWA[2], K. SAITO[1], J. SAWADA[2], & S. NARIMATSU[1]

[1]*Graduate School of Medicine, Dentistry and Pharmaceutical Sciences, Okayama University, 1-1-1 Tsushima-naka, Okayama, 700-8530, Japan, and* [2]*Division of Biochemistry and Immunochemistry, National Institute of Health Sciences, 1-18-1 Kamiyoga, Setagaya-ku, Tokyo, 158-8501, Japan*

(*Received 6 October 2006; revised 2 November 2006; accepted 19 November 2006*)

Abstract

Cytochrome P450 2C19 (CYP2C19) plays an important role in the metabolism of a wide range of therapeutic drugs and exhibits genetic polymorphism with interindividual differences in metabolic activity. We have previously described two CYP2C19 allelic variants, namely *CYP2C19*18* and *CYP2C19*19* with Arg329His/Ile331Val and Ser51Gly/Ile331Val substitutions, respectively. In order to investigate precisely the effect of amino acid substitutions on CYP2C19 function, CYP2C19 proteins of the wild-type (CYP2C19.1B having Ile331Val) and variants (CYP2C19.18 and CYP2C19.19) were heterologously expressed in yeast cells, and their *S*-mephenytoin 4′-hydroxylation activities were determined. The K_m value of CYP2C19.19 for *S*-mephenytoin 4′-hydroxylation was significantly higher (3.0-fold) than that of CYP2C19.1B. Although no significant differences in V_{max} values on the basis of microsomal and functional CYP protein levels were observed between CYP2C19.1B and CYP2C19.19, the V_{max}/K_m values of CYP2C19.19 were significantly reduced to 29–47% of CYP2C19.1B. By contrast, the K_m, V_{max} or V_{max}/K_m values of CYP2C19.18 were similar to those of CYP2C19.1B. These results suggest that Ser51Gly substitution in CYP2C19.19 decreases the affinity toward *S*-mephenytoin of CYP2C19 enzyme, and imply that the genetic polymorphism of *CYP2C19*19* also causes variations in the clinical response to drugs metabolized by CYP2C19.

Keywords: *CYP2C19, genetic polymorphism, CYP2C19*18, CYP2C19*19, S-mephenytoin 4′-hydroxylation*

Correspondence: Dr Shizuo Narimatsu, Graduate School of Medicine Dentistry and Pharmaceutical Sciences, Okayama University 1-1-1 Tsushima-naka, Okayama, 700-8530, Japan. Tel: +81-86-251-7942. Fax: +81-86-251-7942. E-mail: shizuo@pharm.okayama-u.ac.jp

*These authors contributed equally and should be considered joint first authors.

ISSN 0049-8254 print/ISSN 1366-5928 online
DOI: 10.1080/00498250601127038

Introduction

Members of the cytochrome P450 (CYP) superfamily of hemoproteins catalyze the oxidative metabolism of exogenous chemicals such as drugs, carcinogens and toxins, as well as endogenous substances such as steroids and fatty acids (Nelson et al. 1996). CYP2Cs are the major subfamily of CYPs that represent approximately 20% of CYP enzymes in human liver and metabolize a similar proportion of clinically used drugs (Goldstein 2001). The CYP2C subfamily consists of four members in humans (CYP2C8, CYP2C9, CYP2C18 and CYP2C19), and their genes are tandemly located on chromosome 10 (10q24.1–q24.3) (Gray et al. 1995).

CYP2C19 plays important roles in the metabolism of a number of therapeutic drugs such as anti-ulcer drugs, omeprazole and lansoprazole, anti-convulsants, *S*-mephenytoin, anti-diabetic drugs, tolbutamide, and anxiolytic drugs, diazepam (Rendic and Di Carlo 1997). The metabolism of these drugs *in vivo* is known to be polymorphic, and individuals can be divided into an extensive metabolizer (EM) group and a poor metabolizer (PM) group. PMs are characterized by a higher area under the concentration-time curve values of the drugs (Katsuki et al. 1997; Furuta et al. 1999; Qin et al. 1999). For example, PMs show a higher cure rate for gastric and duodenal ulcers by omeprazole (Furuta et al. 1998, 1999; Goldstein 2001). It has been also reported that there are ethnic differences in the frequencies of PMs of CYP2C19 enzyme: 2–5% in Caucasian populations, 2–5% in African populations and 13–25% in Asian populations (Wedlund 2000; Goldstein 2001). These differences are known to be attributed to the genetic polymorphism of the *CYP2C19* gene (Goldstein 2001). Various mutations of the *CYP2C19* gene have been identified from ethnically different populations (http://www.imm.ki.se/CYPalleles/cyp2c19.htm). The PM-related *CYP2C19* polymorphism of oriental populations can be explained by the combination of two-point mutations, *CYP2C19*2* (681G > A, splicing defect) of exon 5 and *CYP2C19*3* (636G > A, Trp212Stop) of exon 4 (de Morais et al. 1994a, 1994b). In Caucasian populations, additionally deficient *CYP2C19* alleles have been subsequently found, although only 2–5% of populations show the PM phenotype (Ferguson et al. 1998; Ibeanu et al. 1998a, 1998b, 1999; Blaisdell et al. 2002; Sim et al. 2006).

Recently, Morita et al. (2004) found another minor allele, *CYP2C19*16* (1324C > T, R442C), at 0.6% frequency in Japanese subjects who had received mephobarbital. With respect to other oriental populations, the defective alleles *CYP2C19*4* (1A > G, no protein) and *CYP2C19*5* (1297C > T, Arg433Trp) were found at low frequencies (<0.5%) in a Chinese population (Xiao et al. 1997; Garcia-Barcelo et al. 1999). More recently, *CYP2C19*17* (−806C > T/−3402C > T) has been reported in the Chinese, Swedish and Ethiopian populations at frequencies of 4–19%) (Sim et al. 2006); however, the other *CYP2C19* alleles (*CYP2C19*6–CYP2C19*15*) have not been detected in oriental populations. Additionally, we also identified two alleles (haplotypes) termed *CYP2C19*18* (986G > A/991A > G, Arg329His/Ile331Val) and *CYP2C19*19* (151A > G/991A > G, Ser51Gly/Ile331Val) in a Japanese population at frequencies of 0.2–0.3%, which cause amino acid substitutions in combination with Ile331Val identified in *CYP2C19*1B* or *CYP2C19*1C* (Table I). Wild-type alleles having 991A > G (Ile331Val) were more frequent compared with alleles with no 991A > G mutation (Fukushima-Uesaka et al. 2005).

The purpose of the current study was to examine the influence of *CYP2C19*18* and *CYP2C19*19* polymorphisms on the catalytic activity of the CYP2C19 enzyme. To achieve this, CYP2C19 cDNAs of wild-type (CYP2C19*1C, encoding CYP2C19.1B protein) and variants (CYP2C19*18 and CYP2C19*19) were constructed, and the corresponding CYP2C19 proteins were heterologously expressed in yeast cells. The enzymatic properties

Table I. Characterization of *CYP2C19* alleles examined.

Allele	Protein	Nucleic acid change	Amino acid substitution
*CYP2C19*1C*[a]	CYP2C19.1B[a]	991A > G	Ile331Val
*CYP2C19*18*	CYP2C19.18	99C > T/986G > A/991 A > G/IVS7-106T > C	Arg329His/Ile331Val
*CYP2C19*19*	CYP2C19.19	99C > T/151 A > G/991 A > G/IVS7-106T > C	Ser51Gly/Ile331Val

[a]Wild-type.

of the CYP2C19 proteins were subsequently examined by kinetic analysis using *S*-mephenytoin as a substrate.

Materials and methods

Materials

CYP2C19*1A cDNA cloned into pBluescript-SK(±) vector (pBluescript/CYP2C19*1A) was kindly provided by Dr Joyce A. Goldstein (National Institute of Environmental Health Sciences, Research Triangle Park, NC, USA). KOD-plus DNA polymerase was purchased from Toyobo (Osaka, Japan); *Hin*dIII was from Takara Bio (Ohtsu, Japan); BigDye terminator cycle sequencing reaction kit v3.1 was from Applied Biosystems (Foster City, CA, USA); pcDNA3.1(+) vector was from Invitrogen (Carlsbad, CA, USA); and QuikChange site-directed mutagenesis kit was from Stratagene (La Jolla, CA, USA). The expression vector pGYR1, which has a GAPDH promoter and includes the yeast NADPH-cytochrome P450 reductase gene (Sakaki et al. 1992), was kindly provided by Dr Yoshihiko Funae (Osaka City University, Osaka, Japan). Yeast nitrogen base was purchased from BD Diagnostics (Franklin Lakes, NJ, USA); Zymolyase 100T was from Seikagaku Corporation (Tokyo, Japan); *S*-mephenytoin was from Toronto Research Chemicals (North York, ON, Canada); 4′-hydroxymephenytoin was from Ultrafine Chemicals (Manchester, UK); NADPH, glucose 6-phosphate and glucose 6-phosphate dehydrogenase were from Oriental Yeast (Tokyo, Japan); rabbit anti-human CYP2C19 antibody was from BD Biosciences (San Jose, CA, USA); peroxidase-conjugated goat anti-rabbit immunoglobulin was from Zymed Laboratories (South San Francisco, CA, USA); and enhanced chemiluminescence-plus reagents were from GE Healthcare Bio-Sciences (Little Chalfont, UK). All other chemicals and reagents used were of the highest quality commercially available.

Construction of CYP2C19 plasmids

CYP2C19*1A cDNA was amplified by polymerase chain reaction from pBluescript/CYP2C19*1A as a template using the forward primer 5′-CCCAAGCTTAA*AAAA*ATGGATCCTTTTGTGGTCC-3′ and the reverse primer 5′-GGAAAGCTTAGGAGCAGCCAGACCATCTGT-3′. *Hin*dIII sites (marked with the solid lines) were introduced to the 5′-end of the start codon and the 3′-end of the stop codon to facilitate subcloning into pGYR1. A yeast consensus sequence (Romanos et al. 1992) (marked in italics) was also introduced upstream of the start codon to achieve a high expression of protein in yeast cells. The PCR product was digested with *Hin*dIII and ligated into the same restriction enzyme site of pcDNA3.1(+), resulting in pcDNA3.1/CYP2C19*1A.

The pcDNA3.1/CYP2C19*1A plasmid was sequenced in both forward and reverse directions using a BigDye terminator cycle sequencing reaction kit v3.1 to confirm that there were no PCR errors. The cDNAs of CYP2C19*1C, CYP2C19*18 and CYP2C19*19 were constructed with a QuikChange site-directed mutagenesis kit according to the manufacturer's instructions using the primers listed in Table II. A mutation for CYP2C19*1C (991A > G) was introduced using pcDNA3.1/CYP2C19*1A as a template, resulting in pcDNA3.1/CYP2C19*1C. Mutations for CYP2C19*18 (991A > G and 986G > A) and CYP2C19*19 (991A > G and 151A > G) were successively introduced using pcDNA3.1/CYP2C19*1C as a template. All CYP2C19 plasmids were sequenced to confirm successful mutagenesis (data not shown). The cDNAs of CYP2C19*1C, CYP2C19*18 and CYP2C19*19 were subsequently subcloned into the pGYR1 yeast expression vector.

Expression of CYP2C19 enzymes

The pGYR1 vectors containing CYP2C19 cDNAs were used to transform *Saccharomyces cerevisiae* AH22 by the lithium acetate method, and yeast transformants were cultivated (Wan et al. 1997). Microsomes from yeast cells were prepared as described previously (Hichiya et al. 2002), and stored at −80°C until use. Protein concentrations were determined by the method of Lowry et al. (1951) using bovine serum albumin as a standard.

Assay for CYP2C19 holo- and apoproteins

Microsomal fractions were diluted to a protein concentration of 10 mg/ml with 100 mM potassium phosphate buffer (pH 7.4) containing 20% (v/v) glycerol and 0.4% (w/v) Emulgen 911, and total functional CYP protein levels were spectrophotometrically measured as reduced carbon monoxide (CO) spectra according to the method of Omura and Sato (1964) using 91 $mM^{-1} cm^{-1}$ as an absorption coefficient for the 450–490 wavelength couple. Total CYP2C19 protein levels of holo- and apoforms in yeast cell

Table II. Primers used for site-directed mutagenesis.

Mutation	Primer	Sequence	Position
991A > G[a]	I331V-F	5′-GATTGAACGTGTC**G**TTGGCAGA AACCGGAGCC-3′	978–1009
	I331V-R	5′-GGCTCCGGTTTCTGCCAA**C**GAC ACGTTCAATC-3′	
986G > A/ (991A > G)[b]	R329H/(I331V)-F	5′-CCAGGAAGAGATTGAAC**A**TGTC GTTGGCAGAAACCGG-3′	969–1005
	R329H/(I331 V)-R	5′-CCGGTTTCTGCCAACGACA**T**GTTC AATCTCTTCCTGG-3′	
151A > G[c]	S51G-F	5′-CCTACAGATAGATATTAAGGATGTC **G**GCAAATCCTTAACC-3′	126–165
	S51G-R	5′-GGTTAAGGATTTGC**C**GACATCCT TAATATCTATCTGTAGG-3′	

Bold and underlined letters indicate the mutation sites introduced by PCR-based mutagenesis.
[a]Primer for CYP2C19*1C, CYP2C19*18 and CYP2C19*19.
[b]Primer for CYP2C19*18.
[c]Primer for CYP2C19*19.

microsomes were determined by immunoblotting. Microsomal fractions (10 μg protein) were separated by 10% sodium dodecyl sulfate-polyacrylamide gel electrophoresis (Laemmli 1970) and electrotransferred to a polyvinylidene fluoride sheet as described by Towbin et al. (1979). The sheet was incubated with rabbit anti-human CYP2C19 antibody (diluted at 1:2000) as the primary antibody and then with peroxidase-conjugated goat anti-rabbit immunoglobulin (diluted at 1:5000) as the secondary antibody. Immunoreactive proteins were visualized with chemifluorescence (enhanced chemiluminescence-plus reagents), and the band densities were relatively determined with Scion Image v4.0 (Scion Corporation, Frederick, MD, USA). The anti-human CYP2C19 antibody recognized a single band in human liver microsomes which co-migrated with microsomes from yeast cells expressing wild-type CYP2C19 in a preliminary study.

Assay for S-mephenytoin 4′-hydroxylation

S-Mephenytoin 4′-hydroxylation was determined by high-performance liquid chromatography (HPLC) as described previously with some modifications (Hanioka et al. 2002). The incubation mixture contained *S*-mephenytoin as a substrate (2–500 μM), microsomes from yeast cells (2 mg protein/ml), 1 mM $NADP^+$, 10 mM glucose 6-phosphate, 2.0 unit/ml glucose 6-phosphate dehydrogenase and 10 mM $MgCl_2$ in 50 mM potassium phosphate buffer (pH 7.4) in a final volume of 500 μl. *S*-Mephenytoin was dissolved in methanol-dimethyl sulfoxide (50:50, v/v). The final concentration of organic solvent (methanol and dimethyl sulfoxide) in the incubation mixture was 1%. The reaction was initiated by the addition of microsomes from yeast cells after pre-incubation at 37°C for 1 min. After incubation at 37°C for 20 min, the reaction was terminated by the addition of 4 ml of dichloromethane. The incubation mixture was spiked with 5 nmol phenobarbital as an internal standard and vigorously vortexed for 2 min. After centrifugation at 2000 *g* for 15 min, the organic phase was evaporated to dryness under a gentle stream of nitrogen at 35°C. The residues were dissolved in 200 μl of methanol-water (50:50, v/v) and analyzed by HPLC. The HPLC system consisted of an L-2130 pump (Hitachi, Tokyo, Japan), an L-2300 column oven (Hitachi) and an L-2400 UV detector (Hitachi) equipped with an Inertsil ODS-80A column (4.6 mm i.d. × 150 mm; GL Sciences, Tokyo, Japan). The column was maintained at 40°C. Data acquisition was accomplished using D-2000 v1.1 software (Hitachi). The product (4′-hydroxymephenytoin) was eluted isocratically with 20 mM potassium dihydrogenphosphate/acetonitrile/methanol (77:17:6, v/v/v) at a flow rate of 1.0 ml/min. UV detection absorbance was recorded at 204 nm. Standard samples were prepared in the same manner as incubation samples. Under these conditions, the retention times of 4′-hydroxymephenytoin, phenobarbital and *S*-mephenytoin were 6.2, 12.7 and 22.0 min, respectively. The detection limit for 4′-hydroxymephenytoin was 5 pmol/assay with a signal-to-noise ratio of 3. The 4′-hydroxymephenytoin formation was linear for at least 40 min in microsomes from livers and yeast cells expressing wild-type CYP2C19. The intra- and inter-day variation coefficients did not exceed 10% in any assay.

Data analysis

Kinetic parameters including K_m and V_{max} for *S*-mephenytoin 4′-hydroxylation were estimated by analyzing Michaelis-Menten plots using Prism v4.0 software (GraphPad Software, San Diego, CA, USA). Intrinsic clearance values were determined as the ratio of V_{max}/K_m. All values are expressed as the mean ± SD of three independent

transfection experiments. Statistical comparisons were performed by one-way analysis of variance with Dunnett's *post-hoc* test using Prism v4.0 software. Differences were considered statistically significant when the p value was <0.05.

Results

Expression of wild-type and variant CYP2C19s in yeast cells

The expression levels of CYP2C19 proteins in microsomal fractions obtained from yeast cells transfected with CYP2C19*1C, CYP2C19*18 and CYP2C19*19 cDNAs were examined by reduced CO difference spectral and immunoblot analyses. As shown in Figure 1(a), the reduced CO difference spectra of CYP2C19.1B, CYP2C19.18 and CYP2C19.19 proteins showed a Soret peak at around 450 nm. The expressed CYP level of CYP2C19.1B was 15.6 pmol/mg of microsomal protein. The level of CYP2C19.18 was 2.0-fold higher than that of CYP2C19.1B, whereas the level of CYP2C19.19 was 65% that of CYP2C19.1B (Figure 1b). The expression levels of wild-type and variant CYP2C19 proteins in yeast cell microsomes were also assessed by immunoblotting which recognized

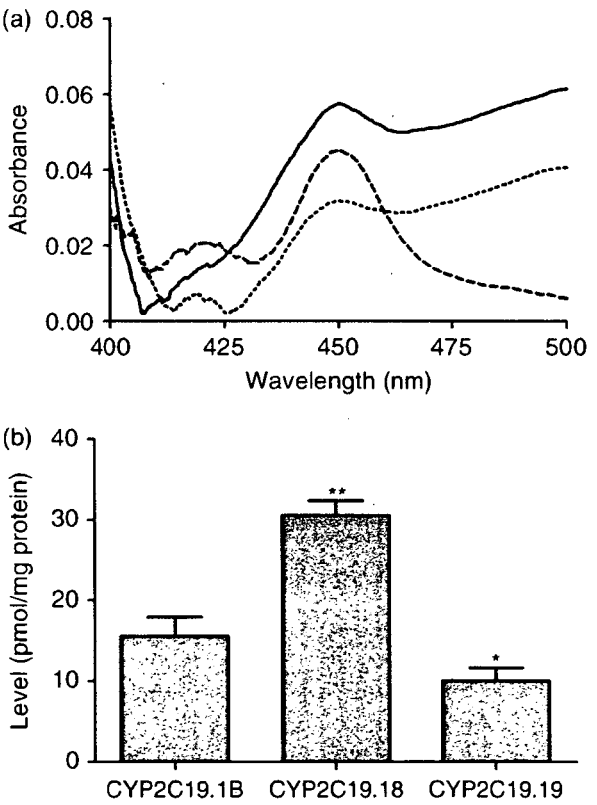

Figure 1. Reduced CO difference spectra of microsomes from yeast cells expressing wild-type and variant CYP2C19s. (a) Representative results of pooled microsomes from three independent preparations. The microsomal protein concentration used was 10 mg/ml. Solid line, CYP2C19.1B; broken line, CYP2C19.18; dotted line, CYP2C19.19. (b) Expression level of CYP2C19 holoprotein. The results are expressed as pmol/mg protein. Each bar represents the mean ± SD of three separate experiments derived from independent preparations. *Significantly different from CYP2C19.1B ($p<0.05$). **Significantly different from CYP2C19.1B ($p<0.01$).

both holo- and apoforms. All constructs except the negative control yielded immunodetectable CYP2C19 protein. The stained bands of CYP2C19.18 and CYP2C19.19 were 171% and 57% of CYP2C19.1B, respectively (Figure 2). The profile for the levels of recombinant protein within yeast cells was reproducible in three independent transfection experiments (data not shown).

Enzymatic properties of wild-type and variant CYP2C19s

S-Mephenytoin 4′-hydroxylation activities in microsomes from yeast cells expressing wild-type and variant CYP2C19s were then examined. Figure 3 shows the activities at low (5 μM) and high (200 μM) substrate concentrations on the basis of microsomal and functional CYP protein levels. *S*-Mephenytoin 4′-hydroxylation activities of CYP2C19.1B at substrate concentrations of 5 and 200 μM on the basis of microsomal and functional CYP protein levels were 9.45 and 62.2 pmol/min/mg protein, and 0.60 and 3.94 pmol/min/pmol CYP, respectively. The activities of CYP2C19.19 at 5 μM substrate were significantly lower (34–54%) than those of CYP2C19.1B in both unit terms. By contrast, the activities of CYP2C19.18 at substrate concentrations of 5 and 200 μM were not significantly different from those of CYP2C19.1B in any unit term. The ratio of activities at substrate concentrations of 5 and 200 μM for CYP2C19.18 on the basis of functional CYP protein

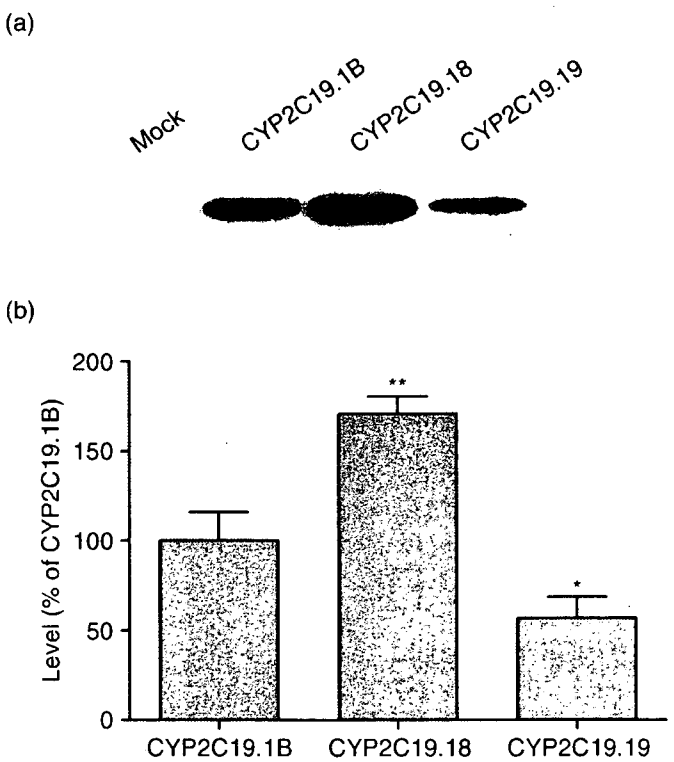

Figure 2. Immunoblotting of microsomes from yeast cells expressing wild-type and variant CYP2C19s. (a) Representative results of pooled microsomes from three independent preparations. The microsomal protein level applied was 10 μg/lane. (b) Expression level of CYP2C19 holo- and apoprotein. The results are expressed as a percentage of the level of CYP2C19.1B. Each bar represents the mean ± SD of three separate experiments derived from independent preparations. *Significantly different from CYP2C19.1B ($p < 0.05$). **Significantly different from CYP2C19.1B ($p < 0.01$).

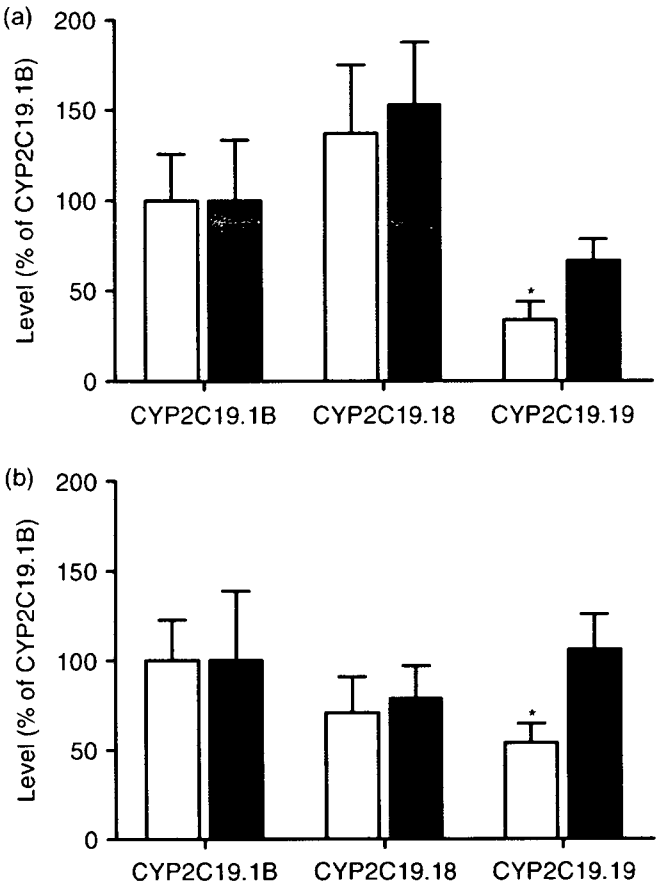

Figure 3. *S*-Mephenytoin 4′-hydroxylation activities in microsomes from yeast cells expressing wild-type and variant CYP2C19s. The results are expressed as a percentage of the activity of CYP2C19.1B. (a) Results on the basis of microsomal protein level. The activities of CYP2C19.1B at 5- and 200 μM substrate concentrations were 9.45 ± 2.43 and 62.2 ± 20.8 pmol/min/mg protein, respectively. (b) Results on the basis of functional CYP protein level. The activities of CYP2C19.1B at 5- and 200 μM substrate concentrations were 0.60 ± 0.14 and 3.94 ± 1.54 pmol/min/pmol CYP, respectively. Each bar represents the mean ± SD of three separate experiments derived from independent preparations. □, 5 μM substrate; ■, 200 μM substrate. *Significantly different from CYP2C19.1B ($p < 0.05$).

level was similar to that for CYP2C19.1B, whereas the relative activity levels of CYP2C19.19 at a substrate concentration of 200 μM was 2.0-fold higher than that at a substrate concentration of 5 μM. No microsomal activity of the negative control was detected at any substrate concentration (data not shown).

To obtain further information on the enzymatic properties of variant CYP2C19s as well as wild-type CYP2C19, kinetic analysis for *S*-mephenytoin 4′-hydroxylation was performed. The nonlinear regression curves of Michaelis-Menten kinetics are shown in Figure 4. The calculated kinetic parameters are summarized in Table III. The K_m value for *S*-mephenytoin 4′-hydroxylation of CYP2C19.1B was 33.5 μM. The K_m value of CYP2C19.19 was significantly higher (3.0-fold) than that of CYP2C19.1B, whereas no significant difference was observed in the K_m values between CYP2C19.1B and CYP2C19.18. The V_{max} and V_{max}/K_m values for *S*-mephenytoin 4′-hydroxylation of CYP2C19.1B on the basis of microsomal protein level were 73.0 pmol/min/mg protein and 2.19 μl/min/mg protein, respectively. When the activities were normalized to CYP holoprotein levels to assess the intrinsic function of wild-type and variant CYP2C19 enzymes, the V_{max} and V_{max}/K_m values

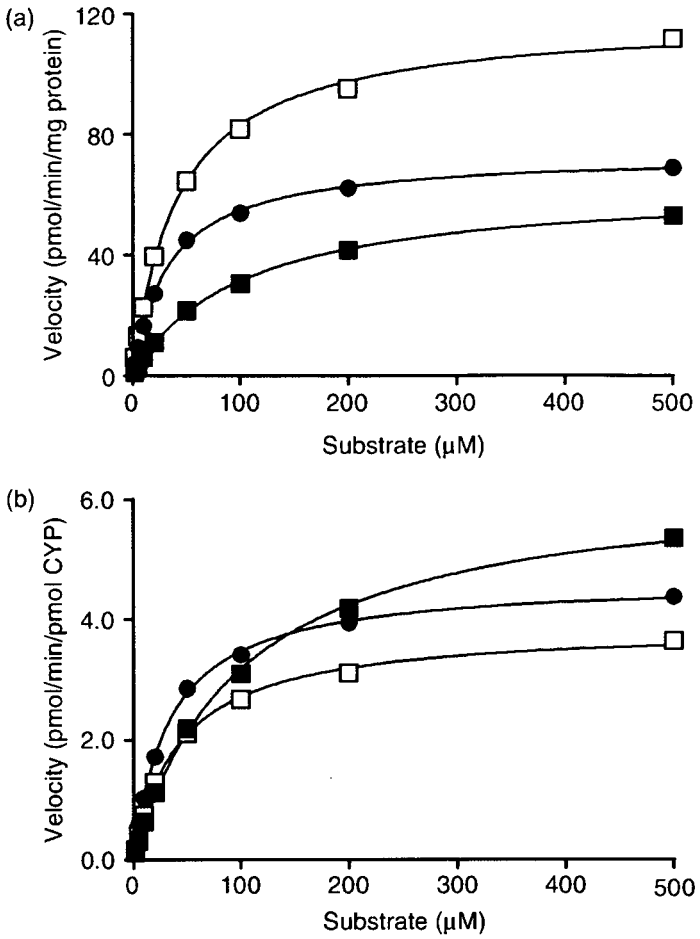

Figure 4. Michaelis-Menten kinetics for *S*-mephenytoin 4′-hydroxylation by microsomes from yeast cells expressing wild-type and variant CYP2C19s. (a) Results on the basis of microsomal protein level. (b) Results on the basis of functional CYP protein level. The substrate concentrations used were 2–500 μM. ●, CYP2C19.1B; □, CYP2C19.18; ■, CYP2C19.19. Each point represents the mean of three separate experiments derived from independent preparations.

of CYP2C19.1B were 4.64 pmol/min/pmol CYP and 138 nl/min/pmol CYP, respectively. The V_{max}/K_m values of CYP2C19.19 on the basis of microsomal and functional CYP protein levels were significantly reduced to 29–47% of CYP2C19.1B, although there were no significant differences in V_{max} values between CYP2C19.1B and CYP2C19.19. By contrast, no significant differences in K_m, V_{max} and V_{max}/K_m values were observed between CYP2C19.1B and CYP2C19.18 in any unit term, although an increasing tendency in the V_{max} value on the basis of microsomal protein level was observed in CYP2C19.18, paralleling the increased holoprotein level (Figure 1).

Discussion

CYP2C19 is a clinically important metabolic enzyme responsible for the metabolism of a number of therapeutic drugs and other xenobiotics (Rendic and Di Carlo 1997). Based on differences in the metabolism of *S*-mephenytoin and other CYP2C19 substrates, individuals